ELSEVIER

Capillary zone electrophoretic determination of C_2–C_{18} linear saturated free fatty acids with indirect absorbance detection

R. Roldan-Assad[a], P. Gareil[b,*]

[a]Laboratoire de Chimie Analytique (URA CNRS 437), Ecole Supérieure de Physique et Chimie Industrielles de La Ville de Paris, 10 Rue Vauquelin, 75231 Paris cedex 05, France
[b]Laboratoire d'Electrochimie et de Chimie Analytique (URA CNRS 216), Ecole Nationale Supérieure de Chimie de Paris, 11 Rue Pierre et Marie Curie, 75231 Paris cedex 05, France

Abstract

The potential of capillary zone electrophoresis for the separation of linear saturated fatty acids in their free form was evaluated. With increasing chain length, difficulties arise from decreasing analyte solubility in aqueous media, increasing occurrence of analyte aggregation and decreasing separation selectivity between successive homologues. A solution was to use electrolytes containing cyclodextrins (CDs) and methanol. The separation of C_2–C_{14} fatty acid homologues differing in only one carbon atom was achieved in less than 10 min using a purely aqueous electrolyte with trimethyl-β-CD as an additive. The separation of C_7–C_{18} homologues was completed in under 20 min with electrolytes containing up to 60% methanol, in addition to the aforementioned CD. In the presence of the CD, analyte solubility is enhanced through the inclusion of the alkyl chain of the acid in the CD cavity, while separation selectivity is improved because the stability constants of the inclusion complexes increase with increasing chain length of the acid. The lack of a suitable chromophore moiety was circumvented through the optimization of indirect absorbance detection conditions. p-Anisate was selected as the chromogenic species. The minimum detectable concentrations are of the order of $(1–2) \cdot 10^{-6}$ mol l^{-1} (0.2–0.5 ppm) and detection linearity was established over at least three orders of magnitude of concentration. The quantitative analysis of a coco oil extract sample is presented, showing results almost identical with those obtained by gas chromatography. Owing to the close values for response factors resulting from the indirect detection principles, a rapid percentage composition can be obtained by corrected peak area normalization.

1. Introduction

During the last decade, the development of capillary electrophoresis (CE) and related electrokinetic techniques has led to interest in widely varying fields of applications involving separations of ionic and non-ionic, polar or apolar, small or large (macro-) molecules. Especially the potential of these techniques for the analysis of ionic surfactant mixtures has recently been addressed and very promising results have emerged for linear alkylsulphonates [1] and alkylsulphates [2], linear and branched alkylbenzenesulphonates [3], and alkyl- and alkylbenzyl quaternary ammonium compounds [4].

Free fatty acids (FFA) constitute an important class of naturally occurring compounds of wide origin which are met as complex mixtures in

* Corresponding author.

animals, plants and even fossil fuels. They differ by their chain length and branching, degree of unsaturation and position and configuration of their double bonds. Some of these natural sources are used as raw materials for the industrial synthesis of various surfactants. There is therefore a stringent demand for their determination in various matrices. However, the separation methods employed often involve a preliminary derivatization step. In the most popular method, gas chromatography (GC) with flame ionization detection, methyl or silyl esters are formed to enhance the analyte volatility prior to introduction on to capillary columns [5–9]. More recently, liquid chromatographic (LC) methods in reversed-phase [5,10–18] or ion-pair modes [19] have also appeared, but the lack of a strongly absorbing chromophore generally precludes the direct use of spectrophotometric detection. Many precolumn derivatization reagents have therefore been proposed to induce sensitivities of more practical interest for absorbance [11,13,15] or fluorescence detection [5,12,14–17]. The determination of amide FFA derivatives by liquid chromatography–mass spectrometry has also been reported [20].

However, a much smaller number of methods that permit the direct determination of FFA in their original form entails the use of specifically designed stationary phases in GC [21,22], nonpolar packed [23,24] or open-tubular capillary columns [25] in supercritical fluid chromatography (SFC) and of refractive index [18], conductivity [19] or low-wavelength UV detection [10] in LC. In addition to the form in which FFA are actually separated, these methods provide slightly different selectivities, viz., for unsaturated species, as a result of their different retention mechanisms. Nevertheless, for compounds having surfactant properties, any technique involving the use of a solid stationary phase is likely to induce undesirable adsorption phenomena. This is why CE techniques performed in free solutions should also be of interest. The first attempts were achieved in capillary isotachophoresis (CITP) and successfully applied to the determination of short-chain ($<C_8$) FFA in formation waters [26] and of C_1–C_{18} linear

FFA in hydrocarbonaceous matrices [27]. Additional benefits lie in the fact that no sample pretreatment is generally required and that conductivity is a fairly sensitive mode of detection in CITP owing to the absence of any background electrolyte in the analyte zone. More attractive approaches are those of capillary zone electrophoresis (CZE) or micellar electrokinetic chromatography (MEKC) which bring about more operational flexibility in addition to their high resolving power. So far, CZE and MEKC separations of FFA have only been reported for chain lengths of $<C_7$ [1,28–31]. The methods described differ in the speed and direction of the electroosmotic flow carrying the analytes simultaneously to electromigration, the use of ionic micelles [31] and in the detection modes, conductivity [28,29] or indirect absorbance [1,30,31].

The purpose of this work was to investigate the separability of long-chain linear saturated FFA by CZE and to assess their detection sensitivity by indirect absorbance. As the chain length of FFA increases, several analytical difficulties arise with such separations owing to the lower and lower analyte solubilities, micelle formation in the separation electrolyte and decreasing separation selectivity between the consecutive homologues. These problems were solved for chain lengths up to C_{18} by optimizing the composition of electrolytes containing methanol and a derivatized cyclodextrin (CD). The conditions for indirect absorbance detection were also studied with regard to linearity and limit of detection. The quantitative aspects are illustrated with the determination of FFA in a coco oil extract sample.

2. Experimental

Experiments were performed with a Perkin-Elmer/Applied Biosystems (ABI, Foster City, CA, USA) Model 270A capillary electrophoresis instrument, equipped with a variable-wavelength absorbance detector. Fused-silica capillaries of 50 μm I.D. from ABI were used in all experiments. The detection window was located 22 cm from the capillary outlet. Samples were intro-

duced in the hydrostatic injection mode using the vacuum depression line of 16.9 kPa on the outlet side of the capillary provided with the instrument. Detector signals were recorded and processed with a Thermo Separation Products/Spectra-Physics Model 4400 integrator (Spectra-Physics, San Jose, CA, USA). The choice of capillary length and the settings for temperature, injection time, separation voltage and detection wavelength are specified according to the sample in the course of the discussion and in the figure captions.

Most of the chemicals used for the electrolytes and the standard samples were of analytical-reagent grade from Aldrich (Milwaukee, WI, USA) or Sigma (St. Louis, MO, USA). Tris–anisate electrolytes were prepared by partially neutralizing Tris base with *p*-anisic acid (both from Aldrich) to the desired pH. The cyclodextrins were gifts from Wacker Chemie (Munich, Germany), except trimethyl-β-CD, which was purchased from Sigma. The sample of coco oil extract was of commercial origin. Water used throughout was of Milli-Q quality (Millipore, Milford, MA, USA).

New capillaries were conditioned by flushing successively with 1 mol l^{-1} sodium hydroxide for 10 min, water for 5 min, 0.5 mol l^{-1} sodium chloride, 6 mmol l^{-1} sodium hydroxide solution for 10 min, water for 5 min and finally with the operating electrolyte for 10 min. With the ABI instrument used, three capillary volumes are displaced in 5 min. Between runs, the capillaries were rinsed with the operating electrolyte for 5 min.

3. Results and discussion

3.1. Overall separation strategy

The first papers dealing with the CZE separation of carboxylic acid homologues suggested conditions that were simply adapted from those derived for UV-transparent small inorganic or organic anions. These conditions generally involved the use of a cationic surfactant to reverse the electroosmotic flow and hence shorten the

analysis time [1,28,29], but this configuration was detrimental to resolution for anionic species. In fact, reversal of the natural cathodic electroosmotic flow is mainly suitable for analytes having their effective mobility in excess, or of the order of the electroosmotic mobility, which is not the case for long-chain FFA. Cathodic electroosmotic flow has already been used by Ackermans et al. [30] for C$_1$–C$_7$ FFA and by Nielen [2] for C$_2$–C$_{12}$ alkylsulphates. Under such conditions, FFA are detected in order of decreasing chain length, i.e., in the reversed order of GC and LC methods, which could be of practical relevance. MEKC was also assessed for the separation of C$_4$–C$_7$ FFA using mixed dodecyl-sulphate–dodecylbenzenesulphonate micelles for indirect absorbance detection [31]. Although a correct resolution was achieved, this approach did not provide satisfactory signal stability and sensitivity. This investigation was therefore concentrated on counter-electroosmotic flow CZE.

As far as detection is concerned, promising results were reported by Huang and co-workers [28,29] with on-column conductivity measurement, but so far this mode has not been easily accessible using commercial instrumentation. In this work, the capability of low-wavelength UV detection was first tested for C$_7$, C$_8$ and C$_9$ FFA with bicine (pH 8.3) and glycine (pH 8.8) buffers at 210 and 200 nm, respectively. However, negative peaks were obtained, indicating that the buffer species absorbed more than the analytes. With a still more transparent buffer such as phosphate–borate (pH 8.9), positive peaks were observed at 200 nm but the sensitivity was poor. Indirect absorbance detection, as already implemented for C$_1$–C$_7$ FFA using a chromogenic species (benzoate) in the electrolyte [1,30], was selected for further optimization.

Another relevant parameter is pH. As linear FFA homologues have almost identical acid–base pK values [32], their separation cannot be based on differences in effective charges. Full ionization of the analytes should rather be sought for separation according to absolute mobilities. A pH range of 8–11 was therefore selected, which also increases the cathodic electroosmotic flow and the solubility of long-chain

FFA. Nevertheless, beyond a certain chain length that needed to be determined, the achievement of a sufficient analyte solubility and the suppression of analyte aggregation require the use of an organic solvent or a specific additive in the electrolyte. Tetrahydrofuran (THF), acetonitrile and methanol were chosen for evaluation. Preliminary solubilization assays in water were also conducted for octadecanoic acid with additives such as sodium dodecyl sulphate, urea, sodium deoxycholate and dimethyl-β-CD. None of these additives succeeded in solubilizing octadecanoic acid at a $2 \cdot 10^{-4}$ mol 1^{-1} concentration, even in basic medium, except the cyclodextrin (CD). This last behaviour suggested the inclusion of the long chain of the acid in the CD cavity. Further assays were subsequently undertaken with other CDs to optimize this effect.

The last aspect to consider is that homologues become increasingly difficult to separate as their chain length increases. As will be shown below, the formation of an inclusion complex between fatty acids and CDs turned out to play a key role in the separation of long-chain FFA, as it allows a selective adjustment of their effective mobility.

3.2. Indirect absorbance detection conditions

For optimized indirect absorbance detection of FFA, the chromophore should preferably bear a negative charge and have a high molar absorptivity for high sensitivity, and its effective mobili-

ty must be close to that of the analytes to reduce electromigration dispersion. The separation electrolyte should not contain any other negatively charged species than the chromophore and its total absorbance should not exceed the upper limit of linear range of Beer's law, for a linear detector response. These conditions also dictate the choice of a cationic buffer pH. The chromogenic species tested are given in Table 1 with the resulting conclusions. Of all the species, p-anisate gave the most satisfactory baseline stability, peak symmetry and sensitivity and was therefore selected for further investigation. The choice of p-anisate concentration and detection wavelength were made with regard to electrolyte absorbance and conductivity. Fig. 1 shows a Beer's law plot obtained by filling the whole capillary with electrolytes of various p-anisate concentrations and measuring the resulting absorbance using the ABI detector. Absorbance appears to be linearly related to p-anisate concentration within the range 0–0.11 absorbance, which is in agreement with results previously reported for similar detector and cell geometries [34]. In addition, the spectrum of p-anisate in a basic methanol–water (50:50, v/v) medium presents a maximum for a wavelength of ca. 245 nm. At this wavelength, the maximum p-anisate concentration permitted for an electrolyte absorbance of 0.11 is only 3 mmol 1^{-1}, which was too low to ensure adequate sample capacity and conductivity. The p-anisate concentration and the wavelength were then fixed at 10 mmol 1^{-1}

Table 1
List of chromophores studied for indirect absorbance detection

Chromophore	Concentration (mmol 1^{-1})	Absolute mobility at 25°C [33] (10^{-5} cm^2 V^{-1} s^{-1})	Detection wavelength (nm)	Remarks
Naphthoate	10		254	Insufficient purity, baseline instability
2-Naphthalenesulfonate	10	31.3	254	Low water solubility
2,3-Dihydroxybenzoate	10	33.0	254	Baseline instability
Picrate	10	31.5	300	Baseline instability
Benzoate	40	33.6	254	Low sensitivity
Chromate	5	81.1	254	Fronting peaks
p-Anisate	10	30.0	270	Adequate baseline stability and sensitivity

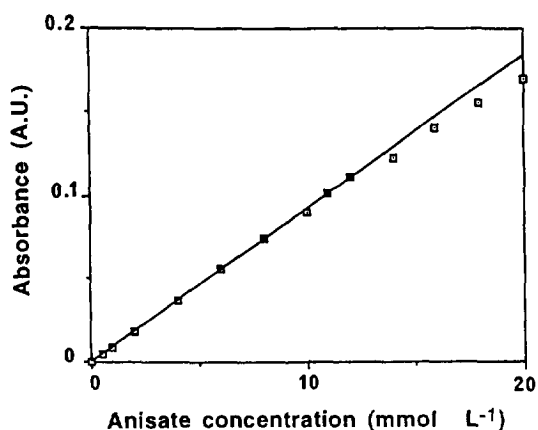Tris electrolyte (pH 8.2) in THF–water (30:70, v/v). Test mixture: linear C_7–C_9 FFA.

Fig. 1. Plot of absorbance versus p-anisate concentration. Optical cell, 50 μm I.D.; 320 μm O.D. fused-silica capillary. Tris–p-anisate buffer (pH 8.1) in methanol–water (50:50, v/v). Wavelength, 270 nm.

and 270 nm, respectively. It was also ascertained that, even if the electrolyte absorbance is kept near to the upper limit of the Beer's law linear range, doubling the p-anisate concentration to 20 mmol l^{-1} while shifting the wavelength to 275 nm resulted, as expected, in a decrease in sensitivity. No other anionic species should be introduced in the electrolyte other than the p-anisate chromophore. Hence setting the p-anisate concentration also sets the electrolyte ionic

strength. Several cationic buffering species were successively tried in the pH range 8–11 in methanol–water (50:50, v/v): Tris (pH 8.1), Ammediol (pH 8.8), ethanolamine (pH 9.5) and cyclohexylamine (pH 10.8). Of these, Tris was selected for further optimization, as it produced the highest baseline stability. The separation of a C_2–C_{14} linear FFA standard mixture obtained with a purely aqueous electrolyte is shown in Fig. 2a. The electropherogram illustrates the progressive loss of resolution for homologues differing by only one carbon atom as the chain length increases, especially in the range of the C_{10}–C_{14} FFA. A marked decrease in peak height also occurs for C_{13} and C_{14} acids, indicating either incomplete solubilization or aggregate formation.

3.3. Sample solubility and selectivity

The achievement of adequate solubility, aggregate breaking and selectivity of long-chain FFA required the use of some organic solvents and/or specific additives. However, the organic solvent content in the electrolyte should be kept low, as an increase in solvent content results in a decrease in electroosmotic mobility, which in turn drastically affects the migration times of anions. Among the solvents tested, THF produced the
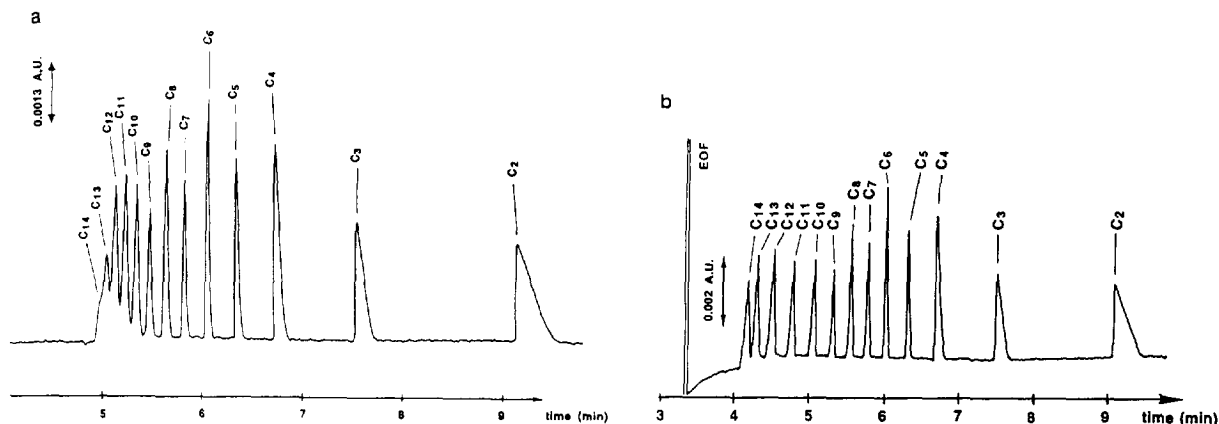

Fig. 2. Effect of addition of a β-CD derivative on the separation of C_2–C_{14} linear FFA standard mixture (0.5 mmol l^{-1} each in methanol) in a purely aqueous electrolyte. Fused-silica capillary, 50 μm I.D. × 72 cm (50 cm to detector). Electrolyte, 20 mmol l^{-1} Tris–10 mmol l^{-1} p-anisate (pH 8.2): (a) without any additive; (b) with 0.75 mmol l^{-1} trimethyl-β-CD added. Applied voltage, 30 kV (I = 3 μA). Temperature, 30°C. Indirect absorbance detection at 270 nm. Hydrodynamic injection for 1 s. EOF = electroosmotic flow.

highest solubilizing power, but a very noisy baseline in the region of anions, even if an unstabilized quality of THF (i.e. free from di-*tert.*-butyl-*p*-cresol) was employed. Acetonitrile was the least detrimental to electroosmotic flow, but solubility was impaired with respect to THF. Finally, methanol led to the best compromise for the most critical FFA in the study, i.e. the C_{14}–C_{18} FFA. Resolution between homologues increased with increasing methanol percentage at the expense of the total analysis time, which became prohibitively long beyond a content of ca. 60%.

In order to minimize the proportion of methanol, the positive effect of CDs was next investigated more deeply. A series of 20 mmol l^{-1} Tris–10 mmol l^{-1} *p*-anisate buffers (pH 8.2) in methanol–water (50:50, v/v) containing 1 mmol l^{-1} of various CDs were examined for solubility and resolution of the C_{16}–C_{18} FFA pair. The CDs tested were the natural α-, β- and γ-CD and the following derivatized CDs: dimethyl-β-CD (degree of substitution, *DS*, 1.8), trimethyl-β-CD (*DS* 3.0), hydroxyethyl-β-CD (*DS* 1.0), hydroxypropyl-β-CD (*DS* 0.9), hydroxypropyl-α-CD (*DS* 0.6) and hydroxypropyl-γ-CD (*DS* 0.6). The best results were obtained with dimethyl- and especially with trimethyl-β-CD. On

increasing the CD concentration, the peak shapes improved continuously, whereas the resolution passed through a maximum for a concentration of the order of 1 mmol l^{-1}. Fig. 2b highlights the improvement in resolution of linear C_{10}–C_{14} FFA achieved when the aqueous electrolyte was supplemented with 0.75 mmol l^{-1} trimethyl-β-CD [35]. It must be emphasized that up to that chain length no organic solvent at all was needed and the electroosmotic mobility is about $60 \cdot 10^{-5}$ cm^2 V^{-1} s^{-1}. The formation of an inclusion complex between FFA and CD causes the effective mobility of the analyte to decrease with increase in CD concentration, as shown in Fig. 3, and this phenomenon becomes more pronounced as the complex stability increases. In fact, using a method described previously [36], the stability constants can easily be derived from the determination of the inflection point on the curves represented in Fig. 3. Table 2 shows that, as expected, the stability of the inclusion complexes increases with increasing hydrophobicity of the guest compounds, i.e., with increasing chain length of the FFA. In the case of partial complex formation, the differences in stability constants between neighbouring homologues result in an increase in the difference between the effective mobilities of these homologues. How-
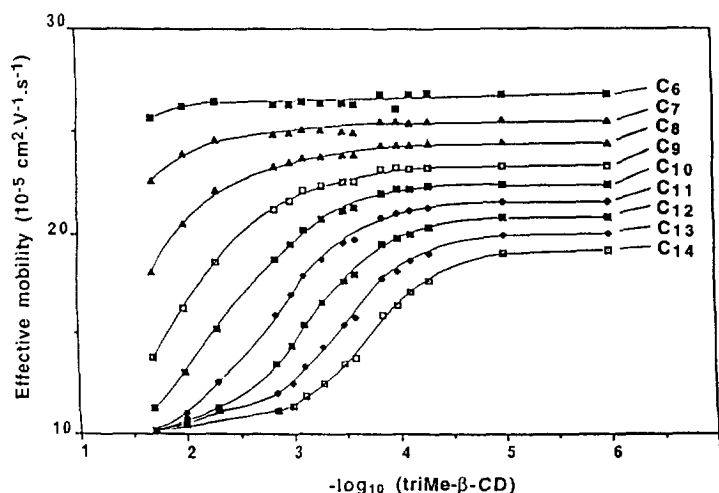

Fig. 3. Variation of the effective mobilities (absolute values) of C_6–C_{14} FFA on addition of trimethyl-β-CD at various concentrations. Operating conditions as in Fig. 2, except for the concentration of the CD. Effective mobilities are calculated as the difference between apparent mobility and electroosmotic mobility.

Table 2
Stability constants, K_f, for inclusion complex formation between linear FFA and trimethyl-β-CD (DS 3.0), determined by CZE

Linear FFA	Log K_f
C_{14}	3.77 ± 0.05
C_{13}	3.58 ± 0.05
C_{12}	3.13 ± 0.05
C_{11}	2.6 ± 0.1
C_{10}	2.2 ± 0.2
C_9	1.9 ± 0.3

Electrolyte, aqueous 20 mmol l^{-1} Tris–10 mmol l^{-1} p-anisate buffer (pH 8.2); temperature, 30°C.

ever, if the CD concentration is increased up to the point where complex formation becomes complete, the effective mobilities of FFA homologues become almost identical owing to the high molecular mass of the CD, and resolution is lost. This phenomenon is reminiscent of what was observed and described for the CZE separation of enantiomers using CDs as chiral additives [37].

Fig. 4 shows the separation of a standard mixture of linear C_7–C_{18} FFA using methanol–water (50:50,v/v) containing 1 mmol l^{-1} trimethyl-β-CD. In this special case, the res-

olution can be considered as too large. The proper methanol concentration can be adjusted according to the qualitative and quantitative compositions of each real sample.

3.4. Total analysis time

The main factors contributing to the total analysis time were electrolyte methanol content, temperature, separation voltage and capillary length. The analysis time is closely related to the amount of methanol needed to produce suitable sample solubility and resolution of the longest FFA. It was also seen that increasing temperature shortened the analysis time significantly, but this caused the resolution to decrease slightly. The temperature of the capillary compartment was set to 30°C. The low ionic strength and conductivity of the electrolyte allowed the separation voltage to be set at 30 kV; the resulting current for a 72 cm × 50 μm I.D. capillary was 3 μA. Fig. 5 shows the impact of simultaneously

Fig. 4. Separation of a C_7–C_{18} linear FFA standard mixture (0.5 mmol l^{-1} each in methanol). Fused-silica capillary, 50 μm I.D. × 72 cm (50 cm to detector). Electrolyte, 20 mmol l^{-1} Tris–10 mmol l^{-1} p-anisate (pH 8.2) containing 1 mmol, l^{-1} trimethyl-β-CD in methanol–water (50:50, v/v). Applied voltage, 30 kV ($I = 3$ μA). Temperature, 30°C. Indirect absorbance detection at 270 nm. Hydrodynamic injection for 1 s.
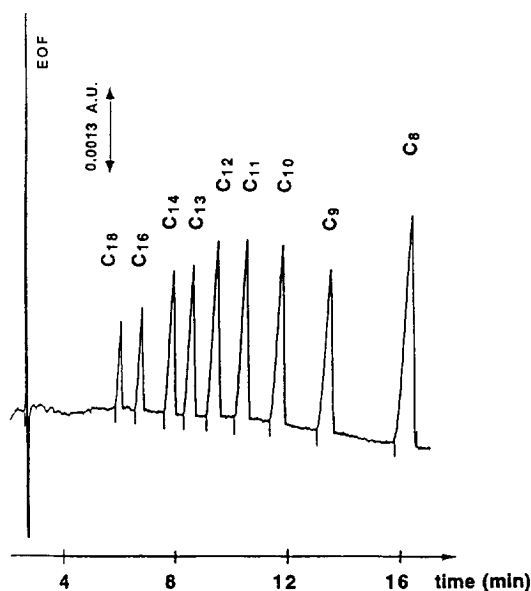
Fig. 5. Separation of a C_8–C_{18} linear FFA reference mixture using optimized capillary length and methanol content. Operating conditions as for Fig. 4, except capillary length, 40 cm (22 cm to detector); electrolyte solvent composition, methanol–water (60:40, v/v) ($I = 4$ μA). The quantitative composition of the reference mixture is given in Table 3, second column.

reducing the total length of the capillary from 72 cm (effective length to the detector cell 50 cm) to 40 cm (effective length 22 cm) and raising the methanol content from 50 to 60%. In spite of the increased methanol content, which brought about more flexibility with respect to the longest FFA, the total analysis time up to the detection of octanoic acid was markedly shortened.

3.5. Quantitative aspects

Special attention was next devoted to the aspects related to method validation, such as detection linearity, precision and detection limits.

A series of samples of a C_8–C_{18} standard mixture of known concentration were first analysed at different dilution factors under the conditions given in Fig. 5, each sample being injected twice. Five successive dilutions differing from one another by a factor of two were performed, so that the range of concentrations covered extended over a factor of 32. The sampling time was kept constant at 1 s, which corresponded to a volume of about 6.4 nl. The plots of migration time-corrected peak areas versus analyte concentration exhibited good linearity over this whole range, as testified by the regression data given in Table 3. No attempt was made to determine the upper concentration limit for signal linearity. Except for octanoic acid, the values determined for the slopes, which corre-

Table 4
Precision expressed as relative standard deviation (R.S.D.) for migration times (t_M) and time-corrected peak areas (A/t_M) of linear FFA

FFA	R.S.D. ($n = 5$) (%)	
	t_M	A/t_M
C_{18}	0.7	6.2
C_{16}	0.8	5.2
C_{14}	0.9	9.1
C_{13}	1.0	6.8
C_{12}	1.0	4.0
C_{11}	1.0	4.0
C_{10}	1.0	2.8
C_9	1.1	6.1
C_8	1.1	7.3

Operating conditions as for Fig. 6, except concentration of the standard mixture used = $C_0/4$.

spond to the sensitivity of the method, increased with increasing alkyl chain length of the FFA, i.e., when the analyte absolute mobility decreased, in agreement with indirect absorbance detection theory [2,30].

A series of five consecutive injections of the C_8–C_{18} standard mixture at a concentration corresponding to the median of the concentration range studied before ($C_0/4$) was next performed for the determination of precision. The results given in Table 4 show that the precisions on migration times were ca. ≤1%, while those on time-corrected peak areas were within the

Table 3
Linear regression data of migration time-corrected peak areas vs. injected concentration of FFA homologue

FFA	C_0 (mmol l^{-1})	Slope (10^5 μV l mol^{-1})	Intercept (μV)	Regression coefficient (R^2)
C_{18}	0.38	1.46	0.25	0.991
C_{16}	0.47	1.21	0.17	0.991
C_{14}	0.80	1.22	0.13	0.996
C_{13}	0.82	1.17	−0.16	0.997
C_{12}	1.18	1.14	0.61	0.997
C_{11}	1.06	1.10	0.67	0.996
C_{10}	1.06	1.03	0.61	0.996
C_9	1.00	0.87	0.33	0.995
C_8	1.00	1.33	0.39	0.999

For each analyte, the range of concentration studied extended from the analyte concentration in the initial standard mixture, C_0, to $C_0/32$. 1 μV corresponds to 1 absorbance unit. Operating conditions as for Fig. 6.

range 3–7%. It can be noted that peak integration was not performed with highly efficient software but simply using a basic integrator.

The minimum detectable concentrations (MDC) were evaluated after a brief determination of the maximum sampling time consistent with still limited extra-column band broadening. The sampling time was raised to 6 s, which corresponded to a volume of 38 nl. A new series of five samples of the C_8–C_{18} standard mixture differing in their dilution factors was injected. The concentrations ranged this time from $C_0/512$ to $C_0/32$, C_0 being the initial concentration of the standard mixture given in Table 3. Linear plots were still obtained in this range for the corrected peak areas versus analyte concentration (so called calibration graphs) with regression coefficients R^2 varying between 0.970 (C_{16}) and 0.998 (C_8). The MDCs were calculated either using peak heights as the analyte concentration producing a signal-to-noise ratio of three, or using corrected peak areas as the concentration producing a signal equal to the intercept of the calibration graph plus three times its standard deviation. The results obtained can be compared in Table 5. The MDCs derived from peak areas were slightly higher than those derived from the peak heights, but no further tendency was observed.

3.6. Qualitative and quantitative analysis of FFA in a coco oil extract

The methods were applied to the determination of FFA in a coco oil extract sample of commercial origin. Using first the purely aqueous electrolyte, peaks corresponding to the even-carbon-number C_6–C_{14} FFA were recognized (Fig. 6), but the presence of heavier FFA could not be established. The same sample was next analysed with the methanol-rich electrolyte. FFA having even-carbon-number chain lengths up to C_{18} were clearly identified, with dodecanoic acid being apparently the major component (Fig. 7). Moreover, no peak other than those of linear C_8–C_{18} FFA was detected, which agrees well with the fact that coco oils are known to mainly contain linear saturated fatty acids.

These last conditions were used to determine the quantitative composition of the coco oil extract. The reference mixture was the standard mixture of C_8–C_{18} FFA diluted twice (concentration $C_0/2$, see Table 3), the concentrations of which were of the same order of magnitude as those in the extract. Undecanoic acid was chosen as the internal standard and was introduced in the sample of coco oil extract at exactly the same concentration as it was in the reference standard mixture. Three methods were implemented to derive the quantitative composition: direct use of the calibration graph (time-corrected peak areas versus analyte concentration, see Table 3) (method A); use of the peak areas obtained with the reference mixture as a single-point calibration and of the ratio of internal standard peak areas for correction of injection conditions (method B); and use of the peak areas obtained with the reference mixture in keeping with the slopes of the calibration graphs and of the ratio of internal standard peak areas (method C). The

Table 5
Minimum detectable concentrations (MDC) of linear FFA determined from peak heights and peak areas

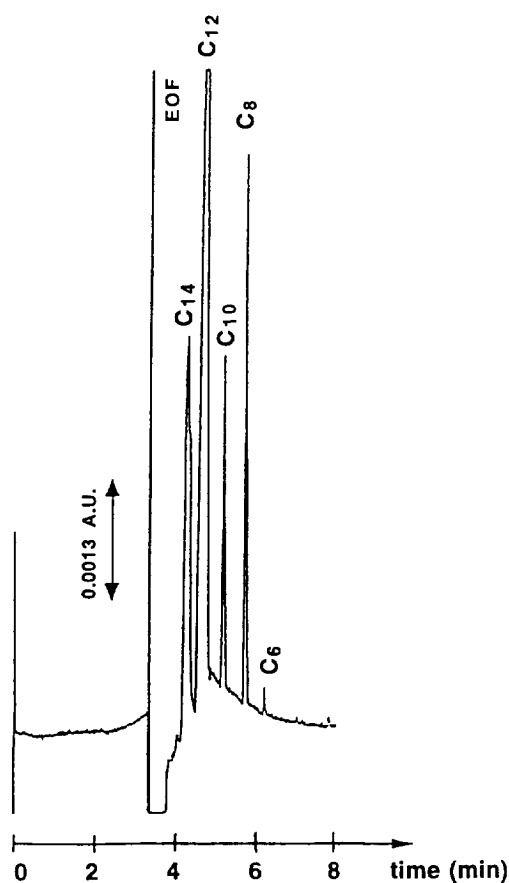| MDC	Units	FFA								
		C_{18}	C_{16}	C_{14}	C_{13}	C_{12}	C_{11}	C_{10}	C_9	C_8
From peak	μmol l^{-1}	0.7	0.6	1.1	2.2	1.4	1.3	1.7	2.4	2.5
heights	ppm	0.2	0.1	0.2	0.5	0.3	0.2	0.3	0.4	0.4
From peak	μmol l^{-1}	2.0	3.6	2.9	2.3	2.2	3.4	2.0	2.4	1.3
areas	ppm	0.6	0.9	0.7	0.5	0.4	0.6	0.3	0.4	0.2

Fig. 6. Electropherogram of the coco oil extract sample dissolved in methanol (260 mg per 100 ml) showing C_6–C_{14} FFA. Operating conditions as for Fig. 2b.
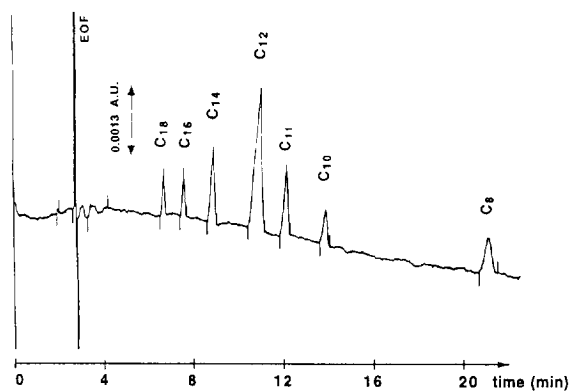

Fig. 7. Electropherogram of the coco oil extract sample dissolved in methanol (65 mg per 100 ml) spiked with undecanoic acid as an internal standard, showing C_8–C_{18} FFA. Operating conditions as for Fig. 5.

Table 6
Molar composition (in mmol l^{-1}) of a commercial coco oil extract, dissolved in methanol (65 mg per 100 ml)

FFA	Method		
	A	B	C
C_{18}	0.180	0.282	0.263
C_{16}	0.223	0.342	0.324
C_{14}	0.468	0.674	0.678
C_{12}	1.333	1.937	1.931
C_{10}	0.169	0.253	0.253
C_8	0.150	0.220	0.230

Method A: direct use of the calibration graphs (see Table 3). Method B: use of the peak areas obtained with the reference mixture as a single-point calibration and of the ratio of internal standard peak areas. Method C: use of the peak areas obtained with the reference mixture in keeping with the slopes of the calibration graphs and of the ratio of internal standard peak areas. Operating conditions as in Fig. 6.

last method allowed us to take advantage of a better estimate of the response factors. Table 6 shows that very close results were obtained by methods B and C, whereas method A leads to markedly lower values, probably because the viscosity of the coco oil extract was higher than that of the standard mixture. This shows that the injection conditions can be an important source of error. Finally, Table 7 gives the composition of the coco oil extract sample in mass percent calculated from the results given in Table 6,

Table 7
Percentage mass composition of the coco oil extract sample calculated from results given in Table 6, method C, and corresponding R.S.D. ($n = 5$), together with the composition of this sample calculated directly from corrected areas (A/t_M) and the average composition of similar samples determined by GC, from supplier's source

FFA	A/t_M (%)	Mass-%	R.S.D. (%)	Mass-% (average, GC)
C_{18}	8.7	10.0	4.3	11[a]
C_{16}	9.0	10.7	2.3	9
C_{14}	18.9	19.8	2.0	18
C_{12}	50.4	49.6	1.3	49
C_{10}	5.9	5.6	4.9	6
C_8	3.1	4.2	3.3	7

[a] Total for $C_{18:0}$, $C_{18:1}$ and $C_{18:2}$ FFA.

method C, with their corresponding relative standard deviations. This composition is not very different from that directly calculated from area normalization, ignoring the response factors. This is a known advantage of indirect absorbance detection [2]. The average composition, determined by GC from the supplier's source, of similar coco oil extracts is also included in Table 7, for the sake of comparison. It should be noted that the present CZE method was not capable of discriminating between the saturated and the mono- and di-unsaturated octadecanoic acids. Apart from this discrepancy and taking into account local and climatic composition variations, it can be considered that a very close agreement was found between the CZE and GC techniques.

4. Conclusion

CZE with indirect absorbance detection has turned out to be a valuable approach for the direct determination of free fatty acids with chain lengths up to C_{18}. Purely aqueous electrolytes can be employed to separate C_2–C_{14} FFA using a CD derivative, while electrolytes containing both 50–60% methanol and the CD are needed to resolve C_8–C_{18} FFA mixtures adequately. CZE appears to be complementary to existing chromatographic methods. While the total analysis times (15–25 min) are similar for the electrophoretic and chromatographic techniques, CZE does not need gradient conditions. The detection order of FFA in CZE is the reverse of that commonly obtained by chromatographic techniques. In the absence of a sample enrichment procedure and with conventional capillaries, the minimum detectable concentrations are at the very low micromolar level (ca. 0.2–0.5 ppm). The linear response range extends over at least three orders of magnitude, from ca. 10^{-6} to 10^{-3} mol l^{-1}, and a rapid mass composition can be obtained from direct corrected area normalization. Sample preparation prior to injection is also less stringent in CZE than in chromatography.

The capability of CZE to resolve long-chain FFA with chain lengths up to C_{18} extends the field of applications of the technique. From the experience gained through this investigation, it seems doubtful that FFA of longer chains can be separated using this approach, since their solubility will require still higher methanol contents, which will be detrimental to inclusion in the CDs, the selectivity and the analysis time. Work is in progress to assess the separability of unsaturated fatty acids.

References

[1] J. Romano, P. Jandik, W.R. Jones and P.E. Jackson, J. Chromatogr., 546 (1991) 411–421.
[2] M.W.F. Nielen, J. Chromatogr., 588 (1991), 321–326.
[3] P.L. Desbène, C. Rosny, B. Desmazières and J.C. Jaquier, J. Chromatogr., 608 (1992) 375–383.
[4] C.S. Weiss, J.S. Hazlett, I.H. Datta and M.H. Danzer, J. Chromatogr., 608 (1992) 325–332.
[5] J.D. Baty, R.G. Willis and R. Tavendale, J. Chromatogr., 353 (1986) 319–328.
[6] W.W. Christie, Gas Chromatography and Lipids, Oily Press. Ayr. 1989.
[7] N.C. Shantha and G.E. Napolitano, J. Chromatogr., 624 (1992) 37–51.
[8] K. Eder, A.M. Reichlmayr-Lais and M. Kirchgessner, J. Chromatogr., 598 (1992) 33–42.
[9] E. Ballesteros, S. Cardenas, M. Gallego and M. Valcarcel, Anal. Chem., 66 (1994) 628–634.
[10] A.K. Batta, V. Dayal. R.W. Colman, A.K. Sinha, S. Sheffer and G. Salen, J. Chromatogr., 284 (1984) 257–260.
[11] H. Miwa, C. Hiyama and M. Yamamoto, J. Chromatogr., 321 (1985) 165–174.
[12] W.W. Christie, HPLC and Lipids, Pergamon Press, Oxford. 1987.
[13] J.F. Lawrence and C.F. Charbonneau, J. Chromatogr., 445 (1988) 189–197.

[14] G. Kargas, T. Rudy, T. Spennetta, K. Takayama, N. Querishi and E. Shrago, J. Chromatogr., 526 (1990) 331–340.

[15] Y. Yasaka, M. Tanaka, T. Shono, T. Tetsumi and J. Katakawa, J. Chromatogr., 508 (1990) 133–140.

[16] J.S. Yoo and V.L. McGuffin, J. Chromatogr., 627 (1992) 87–96.

[17] F. Zonta, B. Stanger, P. Bognoni and P. Masotti, J. Chromatogr., 594 (1992) 137–144.

[18] C.B. Ching, K. Hidajat and M.S. Rao, J. Liq. Chromatogr., 16 (1993) 527–540.

[19] Y. Tsuyama, T. Uchida and T. Goto, J. Chromatogr., 596 (1992) 181–184.

[20] T. Kusaka and M. Ikeda, J. Chromatogr., 639 (1993) 165–173.

[21] K.I. Sakodynsky, G.A. Smolyaninov, V.Y. Zelvensky and N.A. Glotova, J. Chromatogr., 172 (1979), 93–105.

[22] C. de Jong and H.T. Badings, J. High Resolut. Chromatogr., 13 (1990) 94–98.

[23] A. Nomura, J. Yamada, K. Tsunoda, K. Sakaki and T. Yokochi, Anal. Chem., 61 (1989) 2076–2078.

[24] Y. Liu, F. Yang and C.J. Pohl, J. Microcol. Sep., 2 (1990) 245–254.

[25] J.W. King, J. Chromatogr., 28 (1990) 9–14.

[26] T. Barth, Anal. Chem., 59 (1987) 2232–2237.

[27] M. Koval, D. Kaniansky, M. Hutta and R. Lacko, J. Chromatogr., 325 (1985) 151–160.

[28] X. Huang, J.A. Luckey, M.J. Gordon and R.N. Zare, Anal. Chem., 61 (1989) 766–770.

[29] X. Huang, M.J. Gordon and R.N. Zare, J. Chromatogr., 480 (1989) 285–288.

[30] M.T. Ackermans, F.M. Everaerts and J.L. Beckers, J. Chromatrogr., 549 (1991) 345–355.

[31] R. Szücs, J. Vindevogel and P. Sandra, J. High Resolut. Chromatogr., 14 (1991) 692–693.

[32] G. Kortum, W., Vogel and K. Andrussow, Dissociation Constants of Organic Acids in Aqueous Solution, Butterworths, London, 1961.

[33] T. Hirokawa, M. Nishino, N. Aoki, Y. Kiso, Y. Sawamoto, T. Yagi and J.-I. Akiyama, J. Chromatogr., 271 (1983) D1–D106.

[34] F. Foret, S. Fanali, L. Ossicini and P. Bocek, J. Chromatogr., 470 (1989) 299–308.

[35] P. Gareil, R. Roldan-Assad and F. Lelièvre, Analusis, 21 (1993) M35–M38.

[36] P. Gareil, D. Pernin, J.-P. Gramond and F. Guyon, J. High Resolut. Chromatogr., 16 (1993) 195–197.

[37] S.A. Wren and R.C. Rowe, J. Chromatogr., 603 (1992) 235–241.